ADVANCED MATERIALS INTERFACES
www.advmatinterfaces.de

Enhanced Stability of $MAPbI_3$ Perovskite Films with Zirconium Phosphate-Phosphonomethylglycine Nanosheets as Additive

Nadir Vanni, Diletta Morelli Venturi, Eros Radicchi, Giulia Quaglia, Elena Cambiotti, Loredana Latterini, Filippo De Angelis, and Ferdinando Costantino**

Methylammonium lead iodide perovskite ($MAPbI_3$) is today considered the most promising component for highly efficient third generation solar cells. However, the lifetime of the solar devices is strongly affected by the stability of the $MAPbI_3$ films toward humidity, UV irradiation, and temperature. The search for efficient protective additives to be used for building up composite perovskite films with enhanced stability is a topic of great interest in the scientific community. In the present paper, a layered zirconium phosphate-phosphonate based on *N*,*N*-phosphonomethylglycine, exfoliated in thin nanosheets (NS), as additive for the stabilization of $MAPbI_3$ crystalline films toward humidity, UV-irradiation, and temperature changes is applied. Notably, the additive is extremely efficient in preventing degradation of the perovskite film, preserving the optical and structural properties, and avoiding the phase transitions normally observed due to temperature increase.

1. Introduction

Today more than ever is essential for the mankind to search for renewable energy sources to fulfill the global energy demands and mitigate climate changes. In this sense, solar energy is one of the most promising renewable energy sources. In the last 10 years, perovskite solar cells (PSCs) have attracted much attention as a promising innovative photovoltaic technology, possibly contributing to a large scale solar energy production, thanks to their high efficiency and low production costs.[1] Despite their attractive potential, the main drawback of PSCs concerns the durability of the perovskite material, due to instability toward many external factors, such as humidity, oxygen, UV light, and temperature fluctuations,[2,3] thus resulting in lifetime of PSCs of barely 1 year, which do not stand a comparison with silicon solar cell, whose lifetime reaches easily 30 years.[1,4]

Therefore, the stabilization of the perovskite material is clearly one of the most crucial issues to be addressed in order to facilitate the commercialization of this technology. More specifically, the aim is to intervene to reduce the chemical instability limiting the formation of defects present in the perovskite, both of which can speed up the process of degradation induced by external factors.[5]

Several different strategies have been tuned up to meet this goal. One of these focuses on the incorporation of additives directly in the perovskite precursors solution to obtain final materials with enhanced properties. These include, for example, polymers,[6,7] cyclodextrins,[8] fullerenes,[9,10] and inorganic acids.[11,12] In a recent work, Xie et al. reported the use of some phosphonic acids, like 3-Phosphonopropionic acid, as additives and fabricated a PSC with a power conversion efficiency (PCE) of about 21% and enhanced device stability due to the presence of $-PO(OH)_2$ group of the additive, which can establish strong hydrogen bonds, passivating shallow point defects and possibly blocking ion migration.[13]

A different approach consists in coating the perovskite layer with specific materials, to protect it from external factors while maintaining unchanged its properties. Specifically, a coating layer deposited over the perovskite can act as a barrier by

N. Vanni, D. Morelli Venturi, E. Radicchi, G. Quaglia, E. Cambiotti, L. Latterini, F. De Angelis, F. Costantino
Department of Chemistry
Biology and Biotechnologies
Università degli Studi di Perugia
via Elce di Sotto, Perugia (PG) 8-06123, Italy
E-mail: filippo.deangelis@unipg.it; ferdinando.costantino@unipg.it
E. Radicchi
Computational Laboratory for Hybrid/Organic Photovoltaics (CLHYO)
Istituto CNR di Scienze e Tecnologie Chimiche "Giulio Natta" (CNR-SCITEC)
via Elce di Sotto, Perugia (PG) 8-06123, Italy
G. Quaglia, E. Cambiotti, L. Latterini
Nano4Light-Lab
via Elce di Sotto, Perugia (PG) 8-06123, Italy
F. De Angelis
CompuNet
Istituto Italiano di Tecnologia
Via Morego 30, Genova (GE) 16163, Italy

The ORCID identification number(s) for the author(s) of this article can be found under https://doi.org/10.1002/admi.202101888.

DOI: 10.1002/admi.202101888

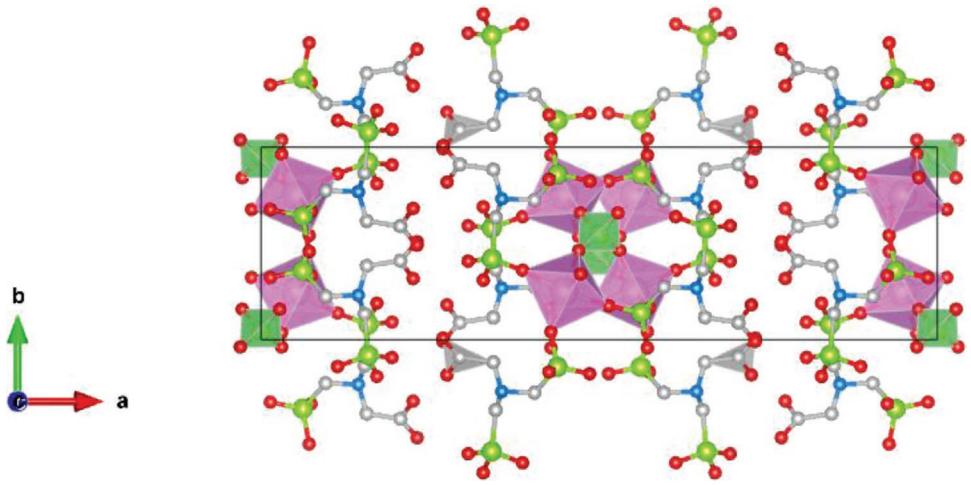

Figure 1. Polyhedral representation of ZPGly viewed along the *c*-axis. ZrO_6 octahedra are in purple, PO_4 tetrahedra are in green. Color codes: P green, C gray, O red, N blue. H-atoms are omitted for clarity.

restricting the diffusion of oxygen and moisture and possibly it should protect also from UV light. For example, an ultrathin layer of Al_2O_3 has been deposited on top of the perovskite layer by atomic layer deposition (ALD), prolonging PSCs lifetime with almost no negative effect on device performance, with 90% of PCE preserved after storage in air for 24 days.[14] Interestingly, when these materials are deposited as nanosheets (NS), they rely on the phenomenon of quantum tunneling to maintain good electron transport properties, while possibly providing moisture protection to the perovskite layer depending on their hydrophobic nature.

Therefore, the choice of an additive or a coating agent capable of improving the stability of the perovskite against detrimental environmental conditions with deposition of thin layers to ensure the electronic conduction by tunnel effect, is a highly desirable goal.

Zirconium phosphonates are a class of compounds already used for a large number of applications, ranging from intercalation,[15] proton conductivity,[16] fillers for nanocomposites,[17] and catalysis.[18] In particular, a mixed phosphate-phosphonate based on *N,N*-bis(phosphonomethyl)glycine (or glyphosine) (L) and with formula $Zr_2(PO_4)(L)_2{\bullet}H_2O$ (hereafter ZPGly)[19] was recently used as support for metal nanoparticles in heterogenous catalyst.[17–22] The prolonged contact with amine solution (such as propylamine, $PrNH_2$) leads to facile exfoliation of the compound thus forming NS of about 3 nm, which is compatible with the stacking of 2 or 3 single layers.[20] Given such desirable properties of ZPGly, in this work, we investigate the possible stabilization of a $MAPbI_3$ perovskite, deposited either on glass or silicon substrate, both by coating ZPGly NS as thin layer and by including them as additives directly in the perovskite precursors solution.

The detailed structure of ZPGly was already reported elsewhere.[19] It consists in packing of complex hybrid layers of about 15 Å of thickness, built from the connection of ZrO_6 octahedra, PO_4 tetrahedra, and PO_3C phosphonate tetrahedra belonging to the glyphosine ligands (**Figure 1**).

The compound also owns three acid protons per unit formula attributable to the carboxylic groups and to P—OH groups. Due to the presence of such acidic protons, the calculated ion exchange capacity (IEC) of the compound is 3.67 meq g^{-1}. Moreover, the carboxylic and amino groups can efficiently coordinate transition metal ions, having a high affinity toward them:[19] in this way, the presence of —COOH and $-PO_3H_2$ free moieties can result in reduced toxicity associated to lead release, coordinating Pb^{2+} ions when perovskites degrade.

ZPGly NS stable dispersion are obtained upon exfoliation of the ZPGly crystalline precursor in *N,N*-dimethylformamide (DMF) and then used as coating agent for crystalline $MAPbI_3$ perovskite deposition or mixed with perovskite precursors solution before crystallization. The samples are tested throughout several experimental techniques, i.e., X-ray powder diffraction (XRPD), thermogravimetric analysis (TGA), differential scanning calorimetry (DSC), scanning electron microscopy (SEM), UV–vis, and luminescence, before and after fast aging treatments in terms of temperature, UV irradiations, relative humidity (RH), and addition of an I^-/I_3^- electrolyte. The addition of Zr phosphonate NS results to strongly enhance the $MAPbI_3$ stability in all the experimental conditions.

2. Results and Discussions

Two different procedures were carried out in order to build the composite by using ZPGly NS gel both as coating agent or by using it as a physical mixture with the $MAPbI_3$ solution (see the Experimental Section). Samples, hereinafter, are named as follow: the crude $MAPbI_3$, **PVK**, $MAPbI_3$ coated with ZPGly NS, **PVK@ZPGly**, and $MAPbI_3$ mixed with ZPGly gel, **MIX.**

XRPD patterns of the **PVK**, of the coverage **PVK@ZPGly**, and of the **MIX** are shown in **Figure 2** The presence of the ZPGly phase does not interfere with the structure and crystallinity of perovskite crystals. The presence of weak reflections in the **PVK@ZPGly** sample, at ≈5° is evidence of the presence of exfoliated ZPGly (see XRD pattern in S1, Supporting Information)

Figure 3 shows the SEM images and the energy-dispersive X-ray spectroscopy (EDX) of the samples. **PVK** a) has grown in the form of highly aligned fibers made by crystals with tetragonal structure. The growth in form of fibers is consistent with the

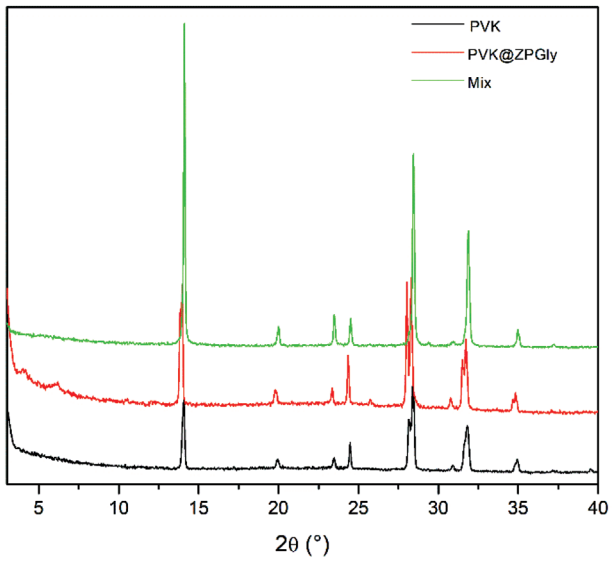

Figure 2. XRPD patterns of **PVK** crystalline deposition (black), **PVK@ZPGly** (red), and **MIX** (green).

data already reported in literature.[23] Figure 3b shows a section of **PVK@ZPGly** composite and from EDX analysis the interface between the two materials can be easily seen. On the contrary, in the **MIX** sample (Figure 3c) the perovskite and ZPGly are mixed evenly, as confirmed by EDX analysis which show a homogeneous distribution of the Zr and Pb in the sample. Additional SEM images are also reported (Figures S2–S4, Supporting Information) TEM images were also collected by dispersing the three samples in EtOH before dropping them on the copper grid precoated with a Formvar film. Despite the dispersion in the solvent leads to an overall separation of the two components, the **ZPGly** nanosheets are clearly visible as thin platelets of 20–200 nm diameter. From TEM it was not possible to measure the lateral thickness of the NS. Perovskite prismatic nanocrystals are also visible as second component both in **MIX** and in the **PVK@ZPGly** systems (Figure S5, Supporting Information). After preparing all the samples, the stability of the protected perovskites against some factors known for threaten the stability of the perovskite alone,[24] namely humidity, UV radiation and temperature was tested. In addition, we conducted tests to check the stability toward redox-active electrolyte I^-/I_3^- as reported in the Supporting Information.

IR spectra of **PVK**, ZPGly, **PVK@ZPGly**, and **MIX** were also collected and reported in Figure S6 (Supporting Information). When ZPGly meets **PVK** (**PVK@ZPGly** and **MIX**) the P—O stretching is not detected, but remarkable peaks are observed in the 1750 and 2750 cm^{-1} region, which could be tentatively assigned to O=P—OR modes. The appearance of these signals supports the establishment of interactions between ZPGly and **PVK**. More importantly, differently from what observed for neat **PVK**, the O—H stretching (3489 cm^{-1}) is not observed for **PVK@ZPGly**, confirming the ability of $Zr_2(PO_4)(L)_2 \cdot H_2O$ to protect the perovskite layer from the humidity adsorption.

2.1. Stability Tests

2.1.1. Relative Humidity (RH) Stability

The samples were placed in a desiccator at 75% RH and were monitored through recording of XRD spectra over time.

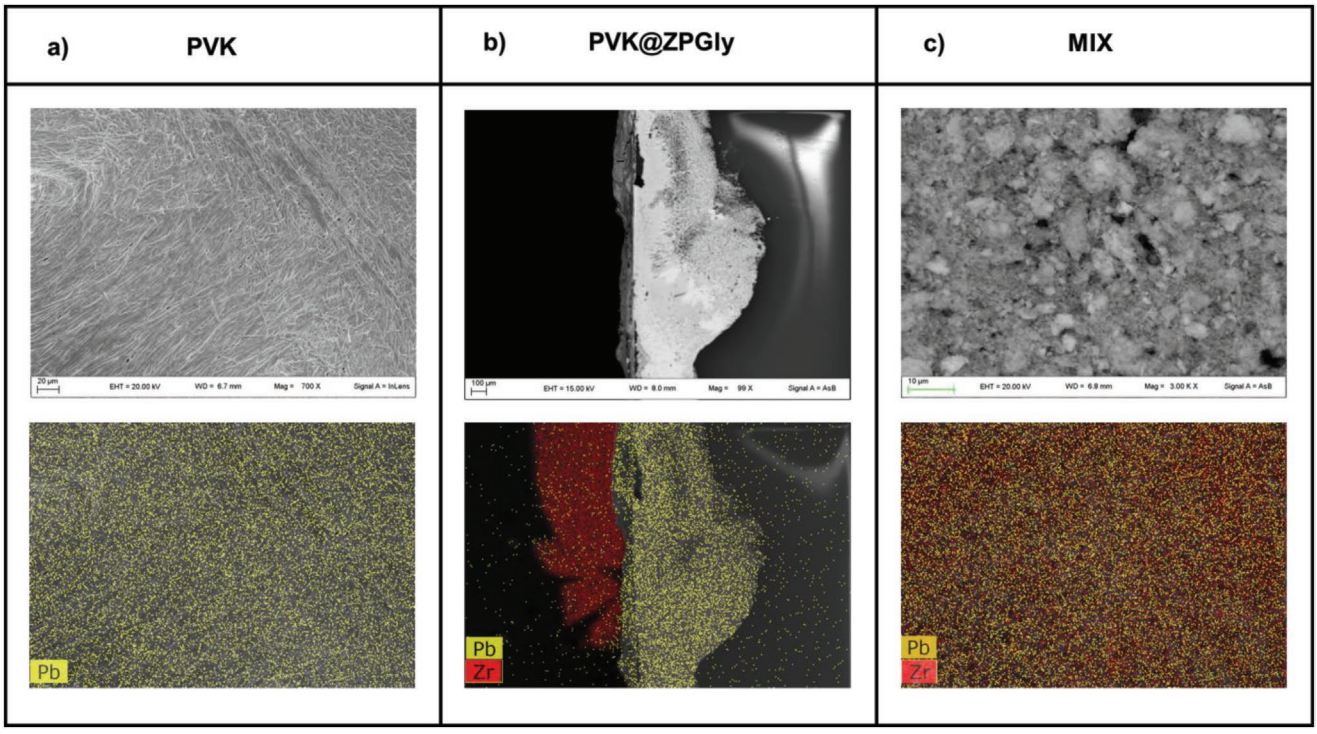

Figure 3. SEM images and relative EDX analysis of a) **PVK**, b) **PVK@ZPGly**, and c) **MIX** samples.

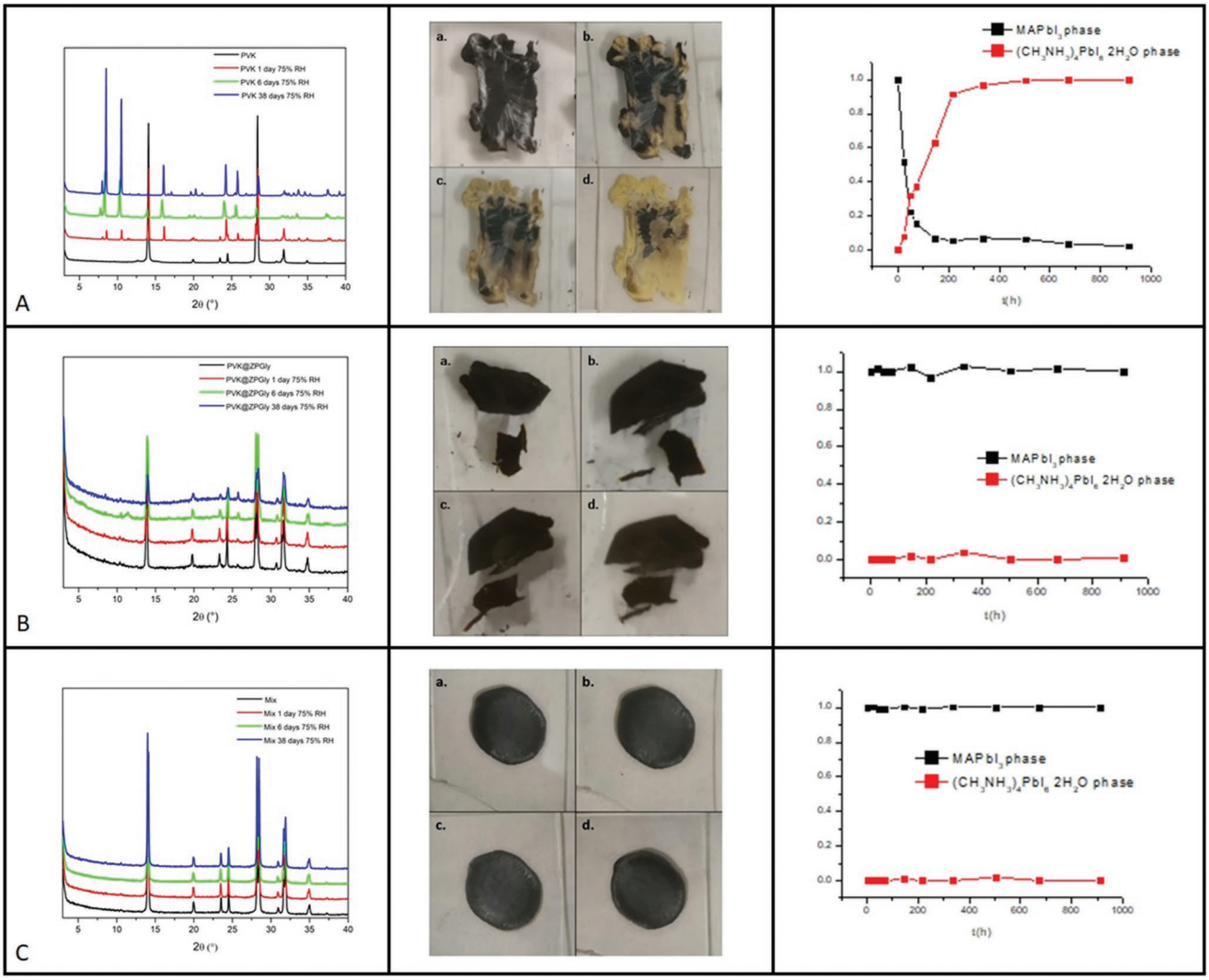

Figure 4. XRD pattern (left), photos (center), and relative intensity trends of $MAPbI_3$ phase and $(CH_3NH_3)_4PbI_6.2H_2O$ (001) and (100) peaks (right) of sample exposed to 75% RH A) **PVK**, B) **PVK@ZPGly**, and C) **MIX**; time 0 (a, black), after 1 day (b, red), 6 days (c, green), and 38 days (d, blue).

The degradation of **PVK**, as a result of the interaction with humidity, is visible to the naked eye (see pictures of the samples in **Figure 4**A) by the evident color changes.

The evident degradation of the **PVK** sample after 1 day in the desiccator can be observed. XRPD patterns of the sample through time are also shown in the figure. The trend over time of the patterns shows the decrease of the intensity of the peak belonging to the pristine perovskite, notably the (001) and (002) at 14.02° and 28.34° 2θ, respectively. On the other hand, some other peaks appeared and increased over time, specifically those at 7.93°, 8.42°, 10.46°, and 16.01°: these peaks cannot be assigned to either the $MAPbI_3$ or PbI_2, but possibly to an intermediate phase. Notably, several studies have been reported in literature about the mechanism of degradation of perovskite due to humidity resulting in the formation of PbI_2. According to these studies,[25,26] the degradation starts with the formation of a hydrate phase of the perovskite with structural formula $(CH_3NH_3)_4PbI_6{\cdot}2H_2O$ from the reaction (1)

$$CH_3NH_3PbI_3 + H_2O \rightarrow (CH_3NH_3)_4\,PbI_6{\cdot}2H_2O \quad (1)$$

The structure of this phase was characterized by Vincent et al. and it consists of an assembly of PbI_6^{4-} octahedra interspersed with $CH_3NH_3^+$ cations and water molecules, with each water molecule forming two hydrogen bonds with two $CH_3NH_3^+$ cations.[27] $(CH_3NH_3)_4PbI_6{\cdot}2H_2O$ is a pale yellow crystalline solid and its XRPD pattern is in line with those we show in Figure 4A. Interestingly, at this level the degradation of perovskite is somewhat reversible: by removing the **PVK** sample from the desiccator, it is possible to see the yellow sample turning black again. To verify the reversibility of the reaction, the **PVK** sample was placed outside the desiccator after 42 days of storage and left at ambient conditions for 10 days. From the XRPD spectra (Figure S7, Supporting Information), we can see that the peaks belonging to the perovskite, that are basically absent from the spectrum of the sample just took out of the desiccator (black line), grow over time, as it is expected since the RH is lower in ambient conditions. Whereas, the peaks of the hydrate phase

decrease, till the point of being completely absent in the case of the sample kept at ambient humidity for 10 days (blue line). Therefore, the **PVK** seems to regenerate but the intensity of the peaks is lower probably due to a partial amorphization.

In contrast to the **PVK**, the sample **PVK@ZPGly** did not show any color change, and it could indicate that the sample has not undergone any degradation. As a confirmation, XRPD pattern are shown in Figure 4B. From the XRPD patterns, the crystalline structure of the perovskite was preserved and no other peaks associated with the hydrate phase or with PbI_2 appeared. All the intensities of peaks are comparable meaning that no amorphization occurred, contrary to the case of **PVK**.

Also, in the case of **MIX**, in images (Figure 4C) the sample does not seem to have suffered any degradation and the XRPD patterns recorded over time confirm it.

2.1.2. UV Irradiation Stability

It has been extensively reported in literature that UV radiation induces degradation of $MAPbI_3$ perovskite resulting in the formation of PbI_2.[27] The test of stability was then carried out, following a previous work by Kajal et al., and exposing the samples to direct UV irradiation at a wavelength of 392 nm (where perovskite crystals absorb, see below) with an intensity of ≈350 mW cm^{-2}.[28] During the experiment, temperature and humidity were maintained at ambient conditions. The samples were monitored for 12 h by recording XRPD patterns. **Figure 5**A (right box) shown mere **PVK** at various time of UV-radiation exposure.

It is evident from both the images and the spectra that the sample had undergone severe degradation after only 12 h.

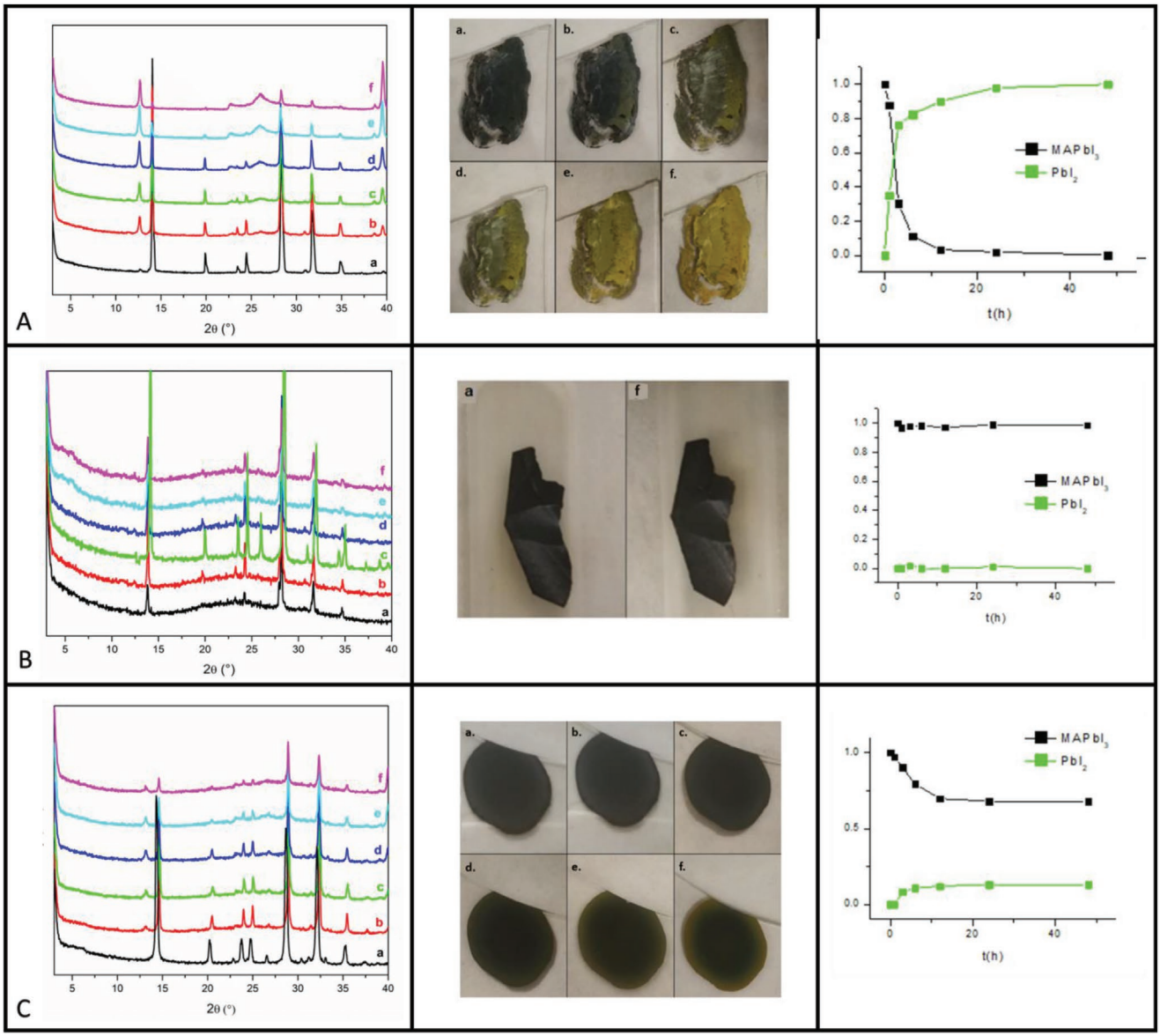

Figure 5. XRPD pattern (left), photos (center) and relative intensity trends of $MAPbI_3$ (001) and PbI_2 (100) peaks (right) of samples exposed to UV rays A) **PVK**, B) **PVK@ZPGly**, and C) **MIX**; time 0 (a, black), time 1 h (b, red), time 2 h (c, green), time 3 h (d, blue), time 6 h (e, cyan), time 12 h (f, magenta).

Peaks of the perovskite, in XRPD patterns (Figure 5A, left box), decrease gradually with the prolonged time of irradiation, instead only after 1 h the peaks belonging to PbI_2, particularly the characteristic peak at 12.64°, become visible and increase. After 12 h of exposition to UV radiation, the **PVK** crystals appeared almost completely degraded to PbI_2.

Contrary to the mere **PVK**, the **PVK@ZPGly** remains stable for all the 12 h as it is shown from both the images and XRPD patterns (Figure 5B) except for the formation of the hydrate phase (pattern c, Figure 5B) which disappear after 3 h.

In XRPD pattern reported in Figure 5A, the appearance of peaks characteristic of PbI_2 can be detected and their increase over time indicates degradation of **PVK**. But comparing the degradation undergone in this sample with the degradation observed in the neat **PVK** sample, a different level of degradation can be hypothesized. While the **PVK** is almost completely degraded, the **MIX** seems to be degraded in a lower degree, as yellow color is observed only on the external part of the crystals. This observation is also confirmed by the variation of relative intensity of the peaks belonging to **PVK** and PbI_2 (Figure 5C, right). After an initial decrease after 4 h, the intenity ratio between the two phases remains unchanged over the entire time of measurement (20 h).

2.1.3. Temperature Stability

The thermal behavior of the mere and protected perovskite was studied through TGA and DSC. First, the TGA heating curves of **PVK**, **ZPGly@PVK**, and **MIX** are shown, see **Figure 6**.

The DSC curve of **PVK** shows a peak around 55 °C corresponding to the exothermic phase transitions from tetragonal to cubic phase.[29]

Instead, the DSC curves of the protected perovskite do not show the phase transition peak suggesting that ZPGly NS, either as coating or mixed phase, might stabilize the tetragonal phase, since the XRPD patterns confirm that the perovskites, mere and protected, were in tetragonal phase before the DSC analysis. Avoiding the phase transitions, and therefore structural instability and lattice distortion caused by temperature fluctuation, can lead to an enhancement of performance of the perovskite[30] (Figure 6, left box).

In order to get more insight in this hypothesis, we collected variable temperature XRPD (VT-XRPD) of the three samples from 25 to 70 °C (5° min^{-1} heating and 10 min equilibration) and back to 25 °C. VT-XRPD patterns of the 20–30° 2-theta region are shown in Figure S8 (Supporting Information). While the **PVK** undergoes the reversible phase transition from cubic to tetragonal over 60 °C, detected by the disappearance (and the successive appearance upon cooling) of the (211) reflection,[31] the **MIX** does not undergo any transition as the (211) peak remained present all over the heating/cooling cycle. Unfortunately, we do not report the results for **ZPGly@PVK** because the phosphonate coating concealed the peaks of perovskite and the phase transition could not be evidenced.

By comparing the TGA curves (Figure 6, right box), no remarkable differences can be seen and the pattern is basically the same for all three samples. The major weight losses are at around 220 and 430 °C and could be assigned to the loss of MAI and PbI_2, respectively.[27] There is only a little weight loss around 125 °C of about 10% already present in the curve of the **PVK** sample and absent in the other two curves.

This weight loss can be assigned to the DMF loss[29] and its absence in the curves of the composites means that ZPGly could facilitate the evaporation of DMF during the synthesis, while in the **PVK** sample a residue of DMF remains.

2.2. Optical Properties of Perovskite Film

UV–vis reflectance spectra of perovskite film in absence and presence of ZPGly (prepared with the two methods described

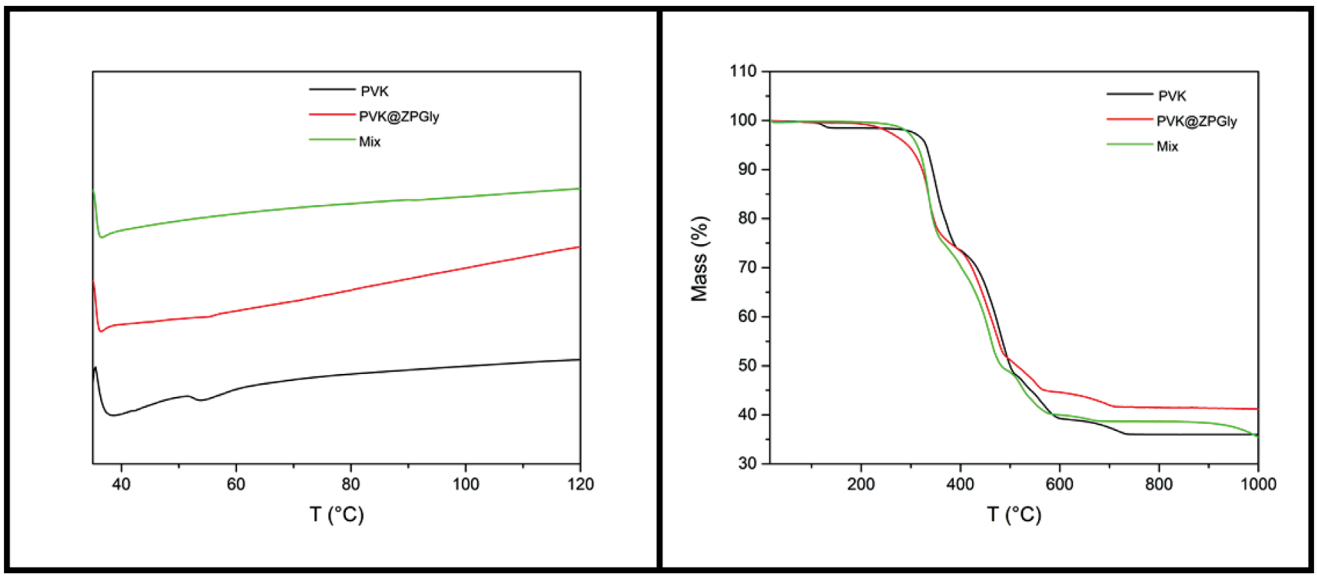

Figure 6. TGA heating curves (right box) and DSC curves (left box) of **PVK** (Black), **PVK@ZPGly** (Red), and **MIX** (Green).

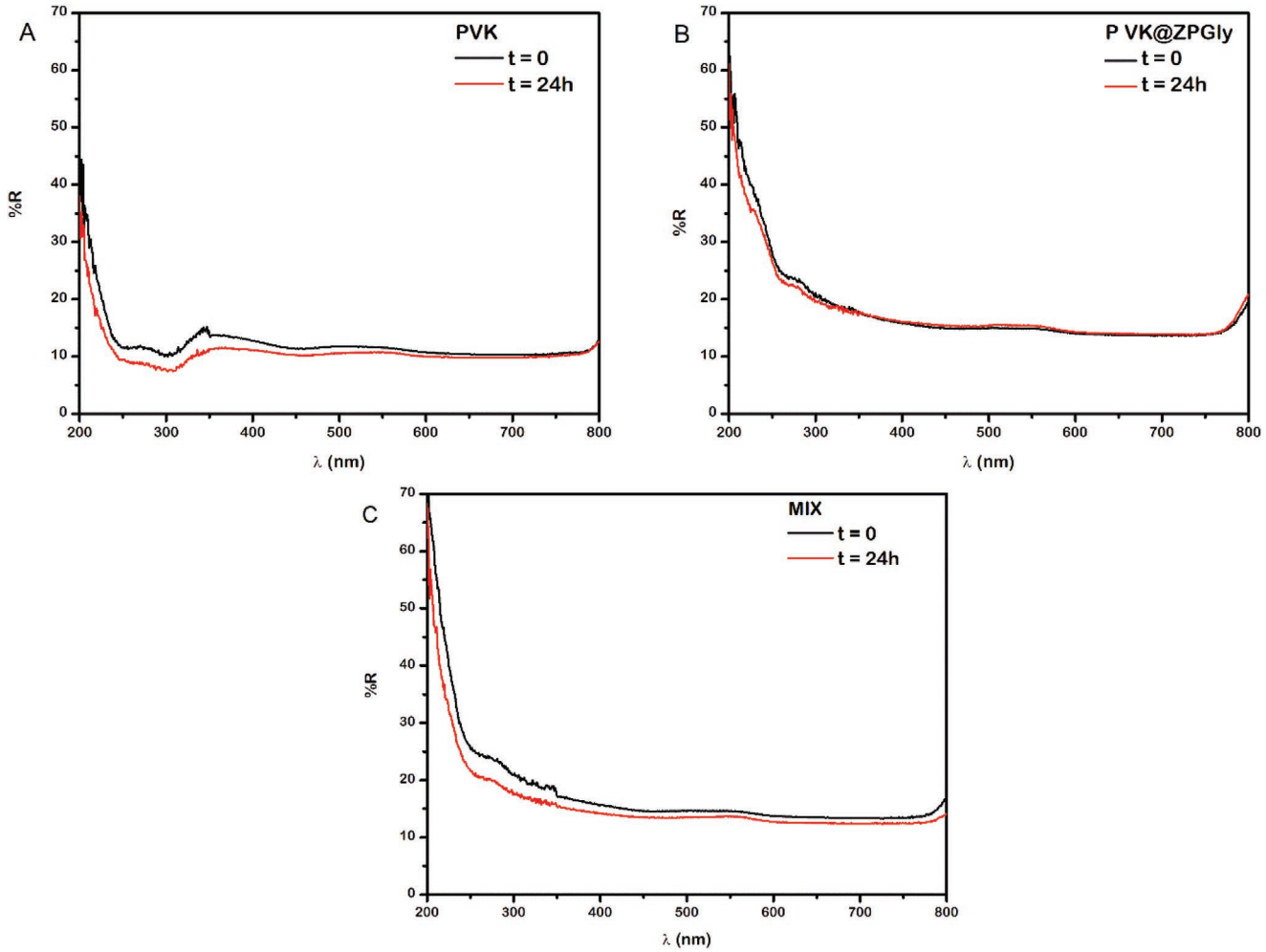

Figure 7. UV–vis reflectance spectra of A) **PVK**, B) **PVK@ZPGly**, and C) **MIX** film registered at time 0 (black) and after 24 h (red).

below), has been collected immediately soon after the preparation and after 24 h later exposure to atmospheric conditions (**Figure 7**). The optical properties of the **PVK@ZPGly** film is not modified after 24 h exposure to air, while **PVK** and the **MIX** film present a detectable alteration in the 250–550 nm region.

The spectra of the samples have been registered after taking the samples in environment with the 75% of RH for 35 days (**Figure 8**). The **PVK** films show an impressive alteration of the electronic properties, as evidenced by the appearance of absorption bands centred at 380 and 425 nm (see black line in Figure 8), attributed to the formation of PbI_3^- and PbI_4^{2-}, respectively.[24,32,33]

This observation documents the alteration of the optical and electronic behaviors of the neat **PVK** films due to its chemical instability caused by humidity. The samples with ZPGly (**PVK@ZPGly** and **MIX**) do not show such an evident modification in the UV–vis spectra, confirming the ability of the inorganic coating to preserve the optical properties of the perovskite, protecting it from damages caused by the chemical transformations induced by humidity.

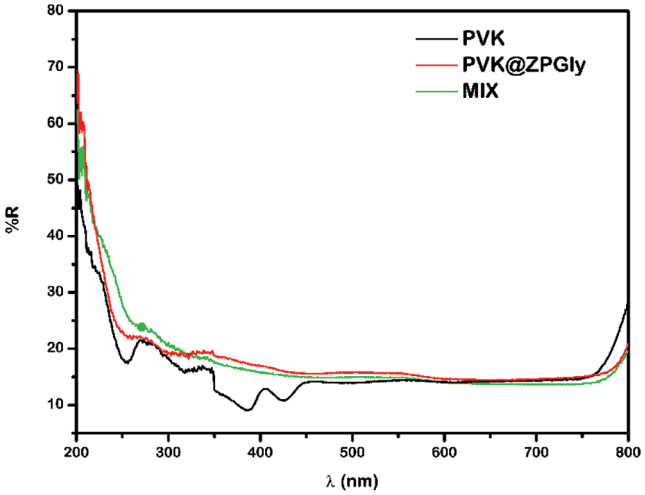

Figure 8. UV–vis reflectance spectra of **PVK** (black), **PVK@ZPGly** (red), and **MIX** (green) kept in an environment with 75% of RH for 35 days.

3. Conclusion

A layered zirconium phosphonate based on glyphosine as building block was employed as additive to $MAPbI_3$ crystalline films deposited on silicon or glass support. The advantage of using such material resided in its high versatility to be obtained as stable dispersion of NS exposing free carboxylic group, having good affinity toward Pb ions and being able to efficiently protect the perovskite deposition without interfering with its structural and optical properties. A second synthetic method was also employed and it was based on mixing the Zr phosphonate gel with the perovskite precursors in order to obtain a physical mixture of the two components. Both methods resulted in a neat improvement of the **PVK** stability toward humidity, temperature, and UV irradiation. XRPD data and UV–vis spectra confirmed the absence of several degradation products normally observed for unprotected **PVK** crystals when aged for more than a month at high RH or exposed for several hours to UV irradiation.

Notably, the coating or mixing with ZPGly prevents the tetragonal to cubic phase transition of $MAPbI_3$ observed around 60 °C which is normally responsible of a general loss of PCE in solar devices due to several reason (density changes causing ruptures, changes in absorption properties, etc.). Future developments will be devoted to the use of the composites in PSC devices in order to test the efficiency and eventually to verify an improved stability according to the results reported in the present paper.

4. Experimental Section

Analytical and Instrumental Procedures–PXRD: PXRD patterns were collected in reflection geometry in the 4–40° 2θ range, with a 40 s $step^{-1}$ counting time and with a step size of 0.016° on a PANalytical X'PERT PRO diffractometer, PW3050 goniometer, equipped with an X'Celerator detector by using the Cu Kα radiation. The long fine focus ceramic tube operated at 40 kV and 40 mA. The XRD graph was plotted with Origin Pro 8.5.

TGA: TGA was performed using a Netzsch STA490C thermoanalyzer under a 20 mL min^{-1} air flux with a heating rate of 10 °C min^{-1}.

DSC: DSC analysis was conducted using an automatic DSC1 (Mettler Toledo Switzerland). Aluminum pans with opened lids were employed in the experiments for all the samples and an empty pan was used as a reference. Samples of 3–5 mg were weighted directly into the aluminum pans and the thermal analyses were conducted at a heating rate of 10 °C min^{-1} from 35 to 120 °C. All runs were carried out under a nitrogen flow of 50 mL min^{-1}.

UV–VIS Spectroscopy: The reflectance spectra were collected by the UV–vis Varian (Cary 4000), equipped with an external integrated sphere DRA900 (diameter of 150 mm), coated by PTFE. A plate of barium sulfate was used as reference.

SEM: Sample morphology was evaluated using a SEM placing the sample on an aluminum stub previously covered with a graphite conductive adhesive. FEG LEO 1525 ZEISS instrument was used.

IR Spectra: The IR spectra in the 4000–400 cm^{-1} frequency range were acquired with an ALPHA compact FT-IR BRUKER, each spectrum was the average of 30 scans with a 2 cm^{-1} resolution, using circular windows of Thallium Bromo-Iodide (KRS5).

TEM images were obtained using a Philips 208 transmission electron microscope. The samples were prepared by putting one drop of an ethanol dispersion of the sample powder on a copper grid precoated with a Formvar film and dried in air.

Chemicals: All chemicals are commercially available and used without further purification. Hydrofluoric acid (HF) and Phosphoric acid (85% wt) (H_3PO_4) were purchased from CarloErba (Italy). Zirconyl chloride ($ZrOCl_2{\bullet}8H_2O$) and Phosphorous acid (H_3PO_3) were purchased from Alfa Aesar. Lead (II) iodide (PbI_2), Methylammonium iodide, DMF, Glycine, Paraformaldehyde (PFA), hydrochloric acid (HCl), and propylamine were purchased from Sigma-Aldrich (Merck).

Synthesis of N,N-Bis(phosphonomethyl)glycine (Glyphosine): Glyphosine was prepared following the Moedritzer–Irani method;[34] glycine (5 g, 67 mmol) were dissolved in 6 M HCl (50 mL),together with H_3PO_3 (11 g, 133 mmol). This mixture was heated to reflux, and paraformaldehyde (8 g, 266 mmol) dispersed in water (10 mL) were slowly added within 2 h. After the last addition of paraformaldehyde, the solution was refluxed for 1 more hour and then the solvent was evaporated. The raw mixture was treated with 2-propanol, yielding a white solid that was filtered under vacuum and dried in an oven at 60 °C; 13.6 g of glyphosine was recovered (Yield = 74%).

Synthesis of $(Zr_2(PO_4))(L)_2{\cdot}H2O$ (ZPGly): The synthesis of ZPGly was achieved as reported in the reference.[19,34] In particular, (2.37 g, 9 mmol) of *N,N*-bis(phosphonometyl)glycine (L) were dissolved in deionized water (93 mL) (0.097 M), and then of phosphoric acid 1 M (6 mL) were added to this solution. $ZrOCl_2{\cdot}8H_2O$ (1.93 g, 6 mmol) were dissolved in HF 2.9 M (20.4 mL, 59 mmol), molar ratio HF/ZrIV = 10. These two solutions were mixed in a 500 mL Teflon bottle and placed in an oven at 90 °C. After 3 days the solid was filtered under vacuum, washed three times with deionized water, and dried at 60 °C for 24 h. The empirical formula was $Zr_2P_5O_{21}C_8N_2H_{19}$ (FW= 816 g mol^{-1}, IEC = 3.67 mmol g^{-1})

Preparation of ZPGly Dispersion: ZPGly (1 g, 1.23 mmol) was suspended in deionized water (108 mL) and then *n*-propylamine 0.1 M (22 mL, 2.2 mmol corresponding to 60% of IEC) were added under vigorous magnetic agitation. A stable dispersion was obtained.

Preparation of ZPGly Gel (DMF): The ZPGly dispersion was ultracentifugated to obtain the exfoliated ZPGly, then it was washed in DMF to exchange the water with DMF. ZPGly gel (DMF) containing 5%wt of ZPGly was obtaining.

Preparation of Perovskite: The synthesis of $MAPbI_3$ (**PVK**) was carried by slow evaporation in DMF. The 1:1 equivalents of MAI (0.954 g, 6 mmol) and PbI_2 (2.766 g, 6 mmol) were mixed in solvent (5 mL), then the solvent was slowly evaporated in an oven at 70 °C. During the solvent evaporation initially a yellow solid was formed and then turned black.[28]

Preparation of Perovskite/ZPGly Composites: *Method one* (**PVK@ZPGly**) a film of ZPGly was prepared by deposition of the solution of exfoliated ZPGly in DMF above a silicon support. When the film was completely dry perovskite grow above the film by drop casting method[34] and following evaporation of the solvent at 70 °C.

Method two (**MIX**) the perovskite precursors solution were mixed together with the ZPGly gel: 1:1 equivalents of MAI (0.954g, 6 mmol), PbI_2 (2.766 g, 6 mmol), and ZPGly gel (DMF) (0.5 g, containing 5%wt of ZPGly) were mixed in solvent (5 mL), were mixed together to obtain a homogeneous solution. After that the solution is deposited on a glass or silicon support and placed at 70 °C to let the DMF evaporate. As a result of the slow evaporation, the film of perovskite and ZPGly is formed with the following composition. 0.8 mg g^{-1} of ZPGly.

Supporting Information

Supporting Information is available from the Wiley Online Library or from the author.

Acknowledgements

The Università degli Studi di Perugia and MIUR are acknowledged for financial support to the project AMIS, through the program

"Dipartimenti di Eccellenza -2018-2022". Authors thank Dr. Andrea Ienco for VT-XRPD measurements and Prof. Paola Sassi for FT-IR spectra.

Open access funding provided by Universita degli Studi di Perugia within the CRUI-CARE Agreement.

Conflict of Interest

The authors declare no conflict of interest.

Data Availability Statement

Research data are not shared.

Keywords

composite perovskite films, solar energy, zirconium phosphonates

Received: October 1, 2021
Published online: November 16, 2021

[1] P. Roy, N. Kumar Sinha, S. Tiwari, A. Khare, *Sol. Energy* **2020**, *198*, 665.
[2] J. S. Manser, M. I. Saidaminov, J. A. Christians, O. M. Bakr, P. V. Kamat, *Acc. Chem. Res.* **2016**, *49*, 330.
[3] J. Bisquert, E. J. Juarez-Perez, *J. Phys. Chem. Lett.* **2019**, *10*, 5889.
[4] G. Grancini, C. Roldán-Carmona, I. Zimmermann, E. Mosconi, X. Lee, D. Martineau, S. Narbey, F. Oswald, F. De Angelis, M. Graetzel, M. K. Nazeeruddin, *Nat. Commun.* **2017**, *8*, 15684.
[5] N. Li, X. Niu, Q. Chen, H. Zhou, *Chem. Soc. Rev.* **2020**, *49*, 8235.
[6] S. Masi, A. Rizzo, F. Aiello, F. Balzano, G. Uccello-Barretta, A. Listorti, G. Gigli, S. Colella, *Nanoscale* **2015**, *7*, 18956.
[7] Y. Guo, K. Shoyama, W. Sato, E. Nakamura, *Adv. Energy Mater.* **2016**, *6*, 1502317.
[8] S. Masi, F. Aiello, A. Listorti, F. Balzano, D. Altamura, C. Giannini, R. Caliandro, G. Uccello-Barretta, A. Rizzo, S. Colella, *Chem. Sci.* **2018**, *9*, 3200.
[9] C.-H. Chiang, C.-G. Wu, *Nat. Photonics* **2016**, *10*, 196.
[10] K. Wang, C. Liu, P. Du, J. Zheng, X. Gong, *Energy Environ. Sci.* **2015**, *8*, 1245.
[11] J. H. Heo, D. H. Song, H. J. Han, S. Y. Kim, J. H. Kim, D. Kim, H. W. Shin, T. K. Ahn, C. Wolf, T.-W. Lee, S. H. Im, *Adv. Mater.* **2015**, *27*, 3424.
[12] R. Mastria, S. Colella, A. Qualtieri, A. Listorti, G. Gigli, A. Rizzo, *Nanoscale* **2017**, *9*, 3889.
[13] H. Xie, Z. Wang, Z. Chen, C. Pereyra, M. Pols, K. Gałkowski, M. Anaya, S. Fu, X. Jia, P. Tang, D. JózefKubicki, A. Agarwalla, H.-S. Kim, D. Prochowicz, X. Borrisé, M. Bonn, C. Bao, X. Sun, S. M. Zakeeruddin, L. Emsley, J. Arbiol, F. Gao, F. Fu, H. I. Wang, K.-J. Tielrooij, S. D. Stranks, S. Tao, M. Grätzel, A. Hagfeldt, M. Lira-Cantu, *Joule* **2021**, *5*, 1246.
[14] X. Dong, X. Fang, M. Lv, B. Lin, S. Zhang, J. Ding, N. Yuan, *J. Mater. Chem. A* **2015**, *3*, 5360.
[15] P. L. Gentili, U. Costantino, R. Vivani, L. Latterini, M. Nocchetti, G. G. Aloisi, *J. Mater. Chem.* **2004**, *14*, 1656.
[16] G. Alberti, M. Casciola, D. Capitani, A. Donnadio, R. Narducci, M. Pica, M. Sganappa, *Electrochim. Acta* **2007**, *52*, 8125.
[17] M. Casciola, *Solid State Ionics* **2019**, *336*, 1.
[18] S. J. I. Shearan, N. Stock, F. Emmerling, J. Demel, P. A. Wright, K. D. Demadis, M. Vassaki, F. Costantino, R. Vivani, S. Sallard, I. R. Salcedo, A. Cabeza, M. Taddei, *Crystals* **2019**, *9*, 270.
[19] A. Donnadio, M. Nocchetti, F. Costantino, M. Taddei, M. Casciola, F. da Silva Lisboa, R. Vivani, *Inorg. Chem.* **2014**, *53*, 13220.
[20] F. Costantino, R. Vivani, M. Bastianini, L. Ortolani, O. Piermatti, M. Nocchetti, L. Vaccaro, *Chem. Commun.* **2015**, *51*, 15990.
[21] F. Costantino, M. Nocchetti, M. Bastianini, A. Lavacchi, M. Caporali, F. Liguori, *ACS Appl. Nano Mater.* **2018**, *1*, 1750.
[22] D. Campoccia, S. Ravaioli, R. Vivani, A. Donnadio, E. Vischini, A. Russo, L. Visai, C. R. Arciola, L. Montanaro, M. Nocchetti, *Materials* **2019**, *12*, 3184.
[23] S. Rahimnejad, A. Kovalenko, S. M. Forés, C. Aranda, A. Guerrero, *ChemPhysChem* **2016**, *17*, 2795.
[24] R. J. Stewart, C. Grieco, A. Larsen, G. S. V. Doucette, J. B. Asbury, *J. Phys. Chem. C* **2016**, *120*, 12392.
[25] J. A. Christians, P. A. Miranda Herrera, P. V. Kamat, *J. Am. Chem. Soc.* **2015**, *137*, 1530.
[26] J. Yang, B. D. Siempelkamp, D. Liu, T. L. Kelly, *ACS Nano* **2015**, *9*, 1955.
[27] B. R. Vincent, K. N. Robertson, T. S. Cameron, O. Knop, *Can. J. Chem.* **1987**, *65*, 1042.
[28] P. Kajal, K. Ghosh, S. Powar, *Applications of Solar Energy*, Springer, Singapore **2018**, pp. 341–364.
[29] A. Dualeh, P. Gao, S. Seok, M. K. Il, Nazeeruddin, M. Grätzel, *Chem. Mater.* **2014**, *26*, 6160.
[30] T. Baikie, Y. Fang, J. M. Kadro, M. Schreyer, F. Wei, S. G. Mhaisalkar, M. Graetzel, T. J. White, *J. Mater. Chem. A* **2013**, *1*, 5628.
[31] F. Jin, J.-T. Ji, C. Xie, Y.-M. Wang, S.-N. He, L. Zhang, Z.-R. Yang, F. Yan, Q.-M. Zhang, *Chin. Phys. B* **2019**, *28*, 076102.
[32] E. Radicchi, E. Mosconi, F. Elisei, F. Nunzi, F. De Angelis, *ACS Appl. Energy Mater.* **2019**, *2*, 3400.
[33] H. J. P. Snaith, *J. Phys. Chem. Lett.* **2013**, *4*, 3623.
[34] K. Moedritzer, R. R. Irani, *J. Org. Chem.* **1966**, *31*, 1603.